

Design and Evaluation of Custom Controller for Fog Screen Device*

Adrian Lozada

Abstract

The overarching goal of the project is the design and evaluation of a fog screen device for improving robot-human communication. The project I was involved in mainly included reverse-engineering the controller of a commercial fog machine, designing a custom controller circuit for autonomous control, testing various configurations to optimize the device's performance, and designing and assembling an improved version of the fog screen device. Key improvements include narrowing the fog and air outlets and incorporating stronger fans. The result shows an increased length of usable fog for projecting images.

1 Introduction

In Human-Robot Interaction (HRI), various communication modalities have been explored [1], including speech and audio [2, 3], gaze [4], visual displays [5], and body languages like gestures and postures [6].

Research efforts have started to leverage augmented reality (AR) to enhance robot communication of non-verbal cues [7, 8, 9, 10, 11, 12, 13], including projected AR works [7, 14] where a robot's navigation paths and manipulation intent were projected onto the ground and table surface, viewable to crowds.

Particularly, AR allows visual overlays situated in a robot's task environment to externalize a robot's internal states. Projector-based AR further improves AR as it offers scalability such that each one in a crowd of people no longer needs to wear AR headsets. However, it is crucial to consider large open environments that lack projectable surfaces, e.g., auditoriums, warehouses, construction sites, and search and rescue scenes. Moreover, projections in some environments may not be legible or visible by humans when humans are not co-located with, e.g., a first responder in a hallway and the robot in a room, or further away from the robot.

While these works [7, 8, 9, 10, 11, 12, 13, 14] improve the understanding of a robot's intent and behaviors like manipulation and navigation using AR, we must solve the problem that some environments lack projectable surfaces.

So, how can we leverage this technology for robot communication when there is no available or suitable (e.g., irregular) surface to project onto? To retain the benefits of projected AR, we propose integrating a fog screen device with a robot to create a mid-air flat display for robots to communicate in environments lacking projectable surfaces. This is particularly beneficial for large-scale open environments, as mentioned before.

Specifically, we already built a fog screen device, Hoverlay II, and tested it on a Fetch robot with a projector (see Fig. 1). We were able to project a human icon onto the mid-air screen to communicate a sign of life to the first responder who might be in a hallway while the robot is searching a room. However, this initial prototype uncovers design flaws/limitations/problems, such as overheating fog machine, small generated fog screen, bulky housing design, weak fans, and airflow getting trapped, which need addressing for efficient and effective integration.

To solve some of the problems, in the summer, I worked with my lab partners and mentor to design and assemble a new fog screen device. The new device included modifications such as narrower fog and air outlets. Furthermore, we upgraded to more powerful fans and a fog machine compared to the initial

*Technical report for the 2024 CRA-WP Distributed Research Experiences for Undergraduates (DREU)



Figure 1: The working prototype of the implemented fog screen device and a projector placed on the base of a Fetch robot. The projected content is a red human icon, which is useful in search-and-rescue scenes to indicate the sign of life of a human victim. It is one of the use cases where no suitable flat surface exists for the robot to project to communicate with humans.

prototype. Additionally, I created a custom circuit board to control the fog machine since we were unable to control the new fog machine via the Fetch robot. Therefore, we opted to build our own control system.

2 Related Work

In robotics, augmented reality has been explored for its potential benefits, showing how AR can enhance interactions [15]. For example, Groechel et al. [16] added two virtual arms to armless robots to express body language to improve perceived emotion, ease of use, and physical presence. Liu et al. [17] used AR to help users better understand a robot’s knowledge structure, e.g., perceived objects, so users can better teach new tasks and understand failures. Hedayati et al. [18] showed that AR visualizations for an aerial robot’s camera capabilities reduced crashes during teleoperation. For a comprehensive review of AR for robotics, we refer readers to the survey by Walker et al. [15].

More related to our work is projected spatial AR where projections are situated in the robot’s operating environment, viewable to a crowd of people without everyone wearing an AR headset. For example, Chadalavada et al. [14] and Covert et al. [10] proposed projecting a mobile robot’s intentions onto the shared floor space with arrows and a simplified map. Han et al. [7] proposed an open-source software and hardware setup for projected AR to popularize this technology in the robotics community. Finally, Walker et al. [8] used AR to help aerial robots convey their motion intents. A user study showed that AR designs, such as NavPoints, Arrows, and Gaze, increased task efficiency and communication clarity.

One limitation of projector-based AR is the reliance on flat surfaces for projection which may not be available in some environments or in scenarios where humans are further away from the robot, thereby undermining the benefits of projected AR for effective communication.

A potential solution is using mid-air displays for projected spatial AR with a robot for communication in these environments. Mid-air fog screen displays create floating surfaces in the air without the need for physical screens. Researchers have delved into different aspects of this technology, e.g., adding gestural interactions [19], developing reconfigurable displays [20, 21, 22, 23], displaying 3D visuals [24] and for multi-user interaction [25], creating a wall-sized walk-through display [26], projecting onto disturbed and deformed screens [27], and improving user engagement with tactile feedback [28, 29].

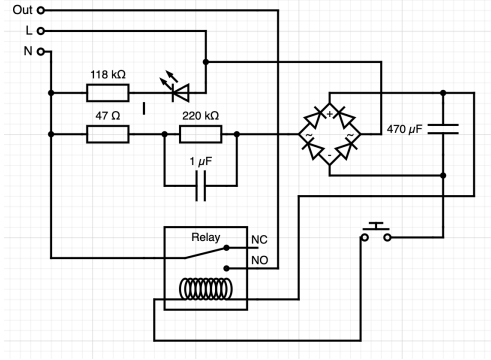


Figure 2: Schematic of the built-in fog machine controller, showing the original control circuit. Key components include resistors (47 Ω , 118 k Ω , and 220 k Ω), a 1 μ F capacitor, a relay, and a bridge rectifier. The circuit is designed to control the power supply to the fog machine, with connections for live (L) and neutral (N) inputs, and output (Out) to the fog machine. The relay operates based on the input signals to manage the fog machine’s power.

Yet, these existing fog screen systems are bulky and are practically impossible to integrate with a robot. For example, Antti et al.’s [29] is over a square meter ($155 \times 105cm$) and Stephen et al.’s [26] is more than 2 meters wide. When integrated, it would rather limit the mobility of a mobile robot or a mobile manipulator. Indeed, there are portable ones, such as the $21 \times 10 \times 7cm$ handheld display [28]) and [20] with a screen width between 6 – 14cm. However, these screen sizes are small for projections to be seen when humans are meters away from the robot.

Finally, Walter [30] developed Hoverlay II, an open-source small ($32.6 \times 27.1 \times 24cm$) fog screen device. Among all related works we surveyed, its small form factor makes it ideal for integrating with robots, and its widescreen allows robots to project onto where humans can still see when farther away from the robot.

However, we do not yet know whether such integration would work perfectly and what improvements roboticists need to make for the robots to communicate.

3 Custom Controller

Before the summer, my lab partners and I developed a prototype of the fog screen device, guided by the design of the Hoverlay II. After assembling the prototype, we conducted tests to evaluate its performance. While the device was able to produce a fog screen, we observed several issues. The most significant problem was the clarity of the fog screen—images projected onto the screen were often blurry. Additionally, the screen’s length was shorter than expected. Seeing these problems, we decided to redesign and assemble a new version of the fog screen device. Our focus shifted to addressing the issues related to fog density and screen length.

To further improve the new design of the Fetch robot needed to control the fog machine autonomously, we developed a custom controller hardware by soldering the necessary components onto a circuit board (Fig. 4). Initially, we faced the problem of there being no documentation on how to interface with the fog machine we bought. To build the custom controller, we disassembled the built-in controller for the remote control to understand its design and inner workings. We found that the built-in controller (Fig. 2), through a DMX port (3), connects a neutral 120V AC wire to the output wire through a relay and a button, thereby closing the circuit. A live wire indicates whether it is ready to produce fog: There is a 3 to 5-minute initial warm-up time upon power connection, and after that, it produces fog for up to 35 seconds. It needs to warm up again, this time for 45 seconds, after each cycle of producing fog for 35 seconds. To begin implementing our

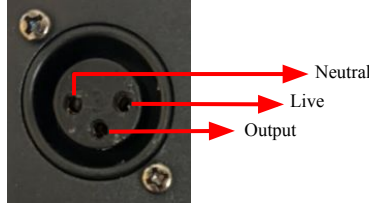


Figure 3: smaller - DMX Port Inputs and Outputs. This Fig. illustrates the DMX port connections for the custom fog machine controller. The labeled connections include Live, Neutral, and Output terminals. This Fig. shows the wiring configuration to interface the DMX port with the fog machine controller.

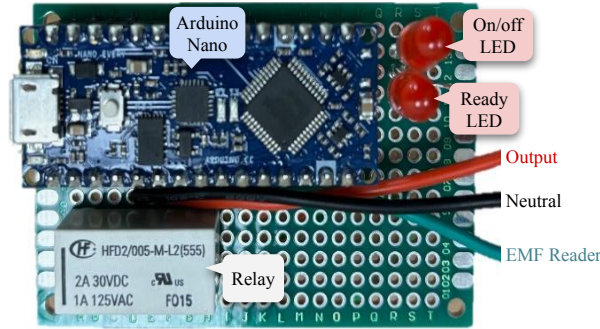


Figure 4: Custom-built fog machine controller circuit. This circuit features an Arduino Nano microcontroller for controlling the fog machine. Key components include the power on/off switch, a ready indicator LED, and an EMF reader for monitoring electromagnetic fields. The relay controls the power supply to the fog machine, with connections for neutral and output.

controller, we gathered an Arduino Nano microcontroller, a relay, and two LEDs to indicate the machine's status. One LED signals when the machine is warm and ready, and the other indicates when it is actively outputting fog, as shown in Fig. 4.

Finally, the fog machine has a DMX cable port (Fig. 3) that controls its operation. This port has three connections: neutral (the port to the left), live (the port to the right), and output (the port in the middle). The neutral and live wires carry a voltage of 120V AC. To control the fog machine, we connect the live wire to the output wire. The fog machine signals its status by setting the live wire high (indicating it is ready) or low (indicating it is not ready). We monitor this status using an LED connected to our Arduino.

Due to the high voltage (120V AC) of the live and neutral wires, direct connection to the Arduino Nano is not feasible. So we used an intermediary relay element that uses an electromagnet to mechanically operate a switch. Specifically, we used a HFD2/005-M L2 latching relay, which stays in its current state (either on or off) until it receives another signal to change. To connect the relay, we wired pin D13 and D12 of the Arduino Nano to the two coil of the relay. Both coils' ground (GND) connections were connected to pin D3 of the Arduino Nano. The fog machine's neutral and output wires were connected to the relay's input and output pins.

4 ROS Node

To enable autonomous control of the fog machine with the Fetch robot, we have created a custom ROS (Robot Operating System) service. This service serves as a bridge between the Fetch robot and the custom controller circuit. The node allows the Fetch robot to send commands to the fog machine and receive status

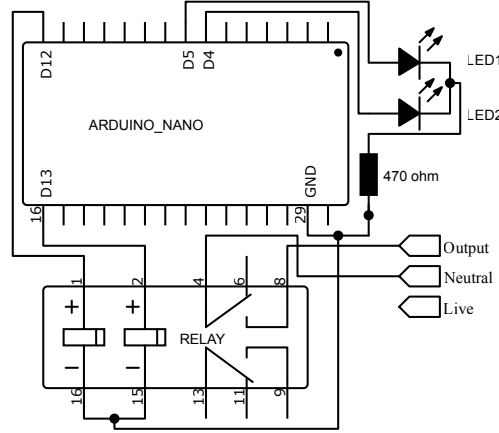


Figure 5: Circuit diagram of our fog machine controller . This Fig. shows the custom-built circuit for controlling the fog machine, featuring an Arduino Nano microcontroller for automation. Key components include the relay for switching the fog machine on and off, the EMF reader for monitoring electromagnetic fields, and the status indicators.

messages.

To facilitate communication between the ROS service and the fog machine, we utilize an Arduino Nano microcontroller. The Arduino Nano is connected to the Fetch robot through a USB serial connection. It is programmed to interpret commands, activate or deactivate the fog machine using a relay, and provide status updates on the fog machine.

5 Evaluation of Prototype

To evaluate the effectiveness of our fog screen device and validate whether our hypotheses to improve it were correct, we conducted a series of experiments. The experiments focus on three modifications to the fog screen device: narrowing the fog outlet, narrowing the air outlet, and increasing the power of the fans. To conduct the experiments, we placed the fog screen device and projector on the base of the Fetch robot. Then, I used a tripod to mount a camcorder to images and videos of the fog screen. We marked where we placed the robot and camera to maintain consistency throughout the experiment. We measured the maximum length of the fog screen by placing the projected image in a position where half of it is blurry, and the other half is clearly visible. We to the measurement of the screen at the point the images turns blurry.

5.1 Narrowing Fog Outlet

The first experiment involved reducing the width of the fog outlet to increase fog density. We hypothesized that a narrower fog outlet would create a denser fog stream, making the screen more suited for projecting images. To achieve this, we designed and 3D printed four flat panels, which were hot glued inside the fog outlet to reduce the width. We designed and printed two sets, one that would reduce the width by 50% and another by 75%.

5.2 Narrowing Air Outlet

In the second experiment, we narrowed the air outlets, which generate a high-pressure air stream that keeps the fog in place and creates a projectable surface. We hypothesized that narrowing the air outlets would

produce stronger air streams, making the fog screen longer. Similar to the fog outlet, we designed and 3D-printed flat panels to reduce the air outlet width by 50% and 75%.

5.3 Using More Powerful Fans

In the final experiment, we tested the effect of using more powerful fans to generate the air stream. We replaced the original fans (rated at 25 Cubic Feet per Minute (CFM)) with stronger fans with a CFM 125. We hypothesized that using more powerful fans would increase the length of the fog screen by generating stronger air stream.

6 Results

Below are some initial preliminary results.

6.1 Narrowing Fog Outlet Result

The results of narrowing the fog outlets showed that narrowing the outlet by 75% increased the fog screen length by seven centimeters. However, narrowing the outlet by 50% didn't affect the length of the fog screen.

6.2 Narrowing Air Outlets Results

The results of narrowing the air outlets showed that decreasing the outlets by 75% decreased the fog screen length by six centimeters, and narrowing the air outlets by 50% decreased the fog screen length by three centimeters.

6.3 Using More Powerful Fans Results

The more powerful fans increased the fog screen length by seventeen centimeters, showing promising results that have been incorporated into the new fog screen device.

7 Designing and Assembling New Iteration

Based on the results of our experiments, we designed and assembled a new iteration of the fog screen device. This version incorporated a 75% reduced fog outlet, and 50% reduced air outlets. We also redesigned the housing to accommodate the more powerful fans while reducing the overall size. To keep the costs down, we used foam boards to build the fog screen device. We plan to evaluate the new iteration under the same conditions as the prototype.

8 Conclusion

This summer, I focused on improving a fog screen device to enhance human-robot communication in environments that lack suitable projection surfaces. The project involved reverse-engineering a fog machine, creating a custom controller for independent operation, and experimenting with different setups to improve the length of the usable fog screen. I found that making certain modifications, such as narrowing the fog and air outlets, increased the length of the usable fog screen. In summary, the work I completed this summer has improved the performance of the fog screen device.

References

- [1] C. Tsiourti, A. Weiss, K. Wac, and M. Vincze, “Designing emotionally expressive robots: A comparative study on the perception of communication modalities,” in *Proceedings of the 5th international conference on human agent interaction*, 2017, pp. 213–222.
- [2] G. Bolano, L. Iviani, A. Roennau, and R. Dillmann, “Design and evaluation of a framework for reciprocal speech interaction in human-robot collaboration,” in *2021 30th IEEE International Conference on Robot & Human Interactive Communication (RO-MAN)*. IEEE, 2021, pp. 806–812.
- [3] F. A. Robinson, O. Bown, and M. Velonaki, “Implicit communication through distributed sound design: Exploring a new modality in human-robot interaction,” in *Companion of the 2020 ACM/IEEE International Conference on Human-Robot Interaction*, 2020, pp. 597–599.
- [4] S. Li and X. Zhang, “Implicit intention communication in human–robot interaction through visual behavior studies,” *IEEE Transactions on Human-Machine Systems*, vol. 47, no. 4, pp. 437–448, 2017.
- [5] E. Sibirtseva, D. Kontogiorgos, O. Nykvist, H. Karaoguz, I. Leite, J. Gustafson, and D. Kragic, “A comparison of visualisation methods for disambiguating verbal requests in human-robot interaction,” in *2018 27th IEEE international symposium on robot and human interactive communication (RO-MAN)*. IEEE, 2018, pp. 43–50.
- [6] H. Knight and R. Simmons, “Laban head-motions convey robot state: A call for robot body language,” in *2016 IEEE international conference on robotics and automation (ICRA)*. IEEE, 2016, pp. 2881–2888.
- [7] Z. Han, J. Parrillo, A. Wilkinson, H. A. Yanco, and T. Williams, “Projecting robot navigation paths: Hardware and software for projected ar,” in *2022 17th ACM/IEEE International Conference on Human-Robot Interaction (HRI)*. IEEE, 2022, pp. 623–628.
- [8] M. Walker, H. Hedayati, J. Lee, and D. Szafr, “Communicating robot motion intent with augmented reality,” in *Proceedings of the 2018 ACM/IEEE International Conference on Human-Robot Interaction*, 2018, pp. 316–324.
- [9] K. Chandan, V. Kudalkar, X. Li, and S. Zhang, “Arroch: Augmented reality for robots collaborating with a human,” in *2021 IEEE International Conference on Robotics and Automation (ICRA)*. IEEE, 2021, pp. 3787–3793.
- [10] M. D. Covert, T. Lee, I. Shinde, and Y. Sun, “Spatial augmented reality as a method for a mobile robot to communicate intended movement,” *Computers in Human Behavior*, vol. 34, pp. 241–248, 2014.
- [11] C. Reardon, K. Lee, J. G. Rogers, and J. Fink, “Communicating via augmented reality for human-robot teaming in field environments,” in *2019 IEEE International Symposium on Safety, Security, and Rescue Robotics (SSRR)*. IEEE, 2019, pp. 94–101.
- [12] R. Newbury, A. Cosgun, T. Crowley-Davis, W. P. Chan, T. Drummond, and E. A. Croft, “Visualizing robot intent for object handovers with augmented reality,” in *2022 31st IEEE International Conference on Robot and Human Interactive Communication (RO-MAN)*. IEEE, 2022, pp. 1264–1270.
- [13] R. T. Chadalavada, H. Andreasson, M. Schindler, R. Palm, and A. J. Lilienthal, “Bi-directional navigation intent communication using spatial augmented reality and eye-tracking glasses for improved safety

- in human–robot interaction,” *Robotics and Computer-Integrated Manufacturing*, vol. 61, p. 101830, 2020.
- [14] R. T. Chadalavada, H. Andreasson, R. Krug, and A. J. Lilienthal, “That’s on my mind! robot to human intention communication through on-board projection on shared floor space,” in *2015 European Conference on Mobile Robots (ECMR)*. IEEE, 2015, pp. 1–6.
 - [15] M. Walker, T. Phung, T. Chakraborti, T. Williams, and D. Szafr, “Virtual, augmented, and mixed reality for human-robot interaction: A survey and virtual design element taxonomy,” *ACM Transactions on Human-Robot Interaction*, vol. 12, no. 4, pp. 1–39, 2023.
 - [16] T. Groechel, Z. Shi, R. Pakkar, and M. J. Matarić, “Using socially expressive mixed reality arms for enhancing low-expressivity robots,” in *2019 28th IEEE International Conference on Robot and Human Interactive Communication (RO-MAN)*. IEEE, 2019, pp. 1–8.
 - [17] H. Liu, Y. Zhang, W. Si, X. Xie, Y. Zhu, and S.-C. Zhu, “Interactive robot knowledge patching using augmented reality,” in *2018 IEEE International Conference on Robotics and Automation (ICRA)*. IEEE, 2018, pp. 1947–1954.
 - [18] H. Hedayati, M. Walker, and D. Szafr, “Improving collocated robot teleoperation with augmented reality,” in *Proceedings of the 2018 ACM/IEEE International Conference on Human-Robot Interaction*, 2018, pp. 78–86.
 - [19] V. Remizova, A. Sand, I. S. MacKenzie, O. Špakov, K. Nyssönen, I. Rakkolainen, A. Kylliäinen, V. Surakka, and Y. Gizatdinova, “Mid-air gestural interaction with a large fogscreen,” *Multimodal Technologies and Interaction*, vol. 7, no. 7, p. 63, 2023.
 - [20] M. A. Norasikin, D. Martinez-Plasencia, G. Memoli, and S. Subramanian, “Sonicspray: a technique to reconfigure permeable mid-air displays,” in *Proceedings of the 2019 ACM International Conference on Interactive Surfaces and Spaces*, 2019, pp. 113–122.
 - [21] M.-L. Lam, B. Chen, K.-Y. Lam, and Y. Huang, “3d fog display using parallel linear motion platforms,” in *2014 International Conference on Virtual Systems & Multimedia (VSMM)*. IEEE, 2014, pp. 234–237.
 - [22] M.-L. Lam, B. Chen, and Y. Huang, “A novel volumetric display using fog emitter matrix,” in *2015 IEEE International Conference on Robotics and Automation (ICRA)*. IEEE, 2015, pp. 4452–4457.
 - [23] M.-L. Lam, Y. Huang, and B. Chen, “Interactive volumetric fog display,” in *SIGGRAPH Asia 2015 Emerging Technologies*, 2015, pp. 1–2.
 - [24] C. Lee, S. DiVerdi, and T. Hollerer, “Depth-fused 3d imagery on an immaterial display,” *IEEE transactions on visualization and computer graphics*, vol. 15, no. 1, pp. 20–33, 2008.
 - [25] Y. Tokuda, M. A. Norasikin, S. Subramanian, and D. Martinez Plasencia, “Mistform: Adaptive shape changing fog screens,” in *Proceedings of the 2017 CHI Conference on Human Factors in Computing Systems*, 2017, pp. 4383–4395.
 - [26] S. DiVerdi, I. Rakkolainen, T. Höllerer, and A. Olwal, “A novel walk-through 3d display,” in *Stereoscopic Displays and Virtual Reality Systems XIII*, vol. 6055. SPIE, 2006, pp. 428–437.
 - [27] K. Otao and T. Koga, “Mistflow: a fog display for visualization of adaptive shape-changing flow,” in *SIGGRAPH Asia 2017 Posters*, 2017, pp. 1–2.

- [28] A. Sand, I. Rakkolainen, P. Isokoski, R. Raisamo, and K. Palovuori, “Light-weight immaterial particle displays with mid-air tactile feedback,” in *2015 IEEE International Symposium on Haptic, Audio and Visual Environments and Games (HAVE)*. IEEE, 2015, pp. 1–5.
- [29] A. Sand, V. Remizova, I. S. MacKenzie, O. Spakov, K. Nieminen, I. Rakkolainen, A. Kylliäinen, V. Surakka, and J. Kuosmanen, “Tactile feedback on mid-air gestural interaction with a large fogscreen,” in *Proceedings of the 23rd International Conference on Academic Mindtrek*, 2020, pp. 161–164.
- [30] M. Walter, “Hoverlay ii open hardware interactive midair screen,” <https://hackaday.io/project/205-hoverlay-ii>, 2014.